JACS
JOURNAL OF THE AMERICAN CHEMICAL SOCIETY
Article
pubs.acs.org/JACS

Single Domain Metallothioneins: Supermetalation of Human MT 1a

Duncan E. K. Sutherland, Mathew J. Willans, and Martin J. Stillman*

Department of Chemistry, University of Western Ontario, London, Ontario N6A 5B7, Canada

ABSTRACT: Metallothioneins are a family of small, cysteine rich proteins that have been implicated in a range of roles including toxic metal detoxification, protection against oxidative stress, and as metallochaperones involved in the homeostasis of both essential zinc and copper. We report that human metallothionein 1a, well-known to coordinate 7 Zn^{2+} or Cd^{2+} ions with 20 cysteinyl thiols, will bind 8 structurally significant Cd^{2+} ions, leading to the formation of the supermetalated Cd_8-$\beta\alpha$-rhMT 1a species, for which the structure is a novel single domain. ESI−mass spectrometry was used to determine the exact metalation status of the $\beta\alpha$-rhMT. The derivative-shaped CD envelope of Cd_7-$\beta\alpha$-rhMT [peak extrema (+) 260 and (−) 239 nm] changed drastically upon formation of the Cd_8-$\beta\alpha$-rhMT with the appearance of a sharp monophasic CD band centered on 252 nm, a feature indicative of the loss of cluster symmetry. The structural significance of the eighth Cd^{2+} ion was determined from a combination of direct and indirect ^{113}Cd nuclear magnetic resonance (NMR) spectra. In the case of Cd_8-$\beta\alpha$-rhMT, only four peaks were observed in the direct ^{113}Cd NMR spectrum. Significantly, while both of the isolated domains can be supermetalated forming Cd_4-β-rhMT and Cd_5-α-rhMT, Cd_8-$\beta\alpha$-rhMT and not Cd_9-$\beta\alpha$-rhMT was observed following addition of excess Cd^{2+}. We propose that both domains act in concert to coordinate the eighth Cd^{2+} atom, and furthermore that this interaction results in a coalescence of the two domains leading to collapse of the two-domain structure. This is the first report of a possible single-"superdomain" metallothionein structure for Zn^{2+} and Cd^{2+} binding mammalian proteins. A computational model of a possible single-domain structure of Cd_8-$\beta\alpha$-rhMT is described.

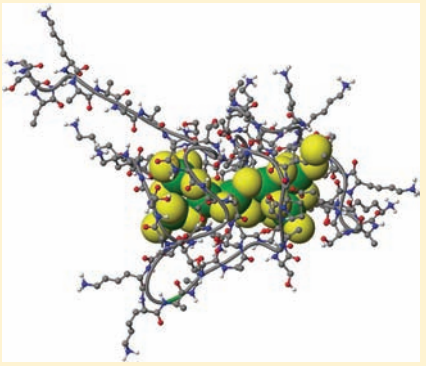

INTRODUCTION

Metallothioneins (MTs), first isolated by Margoshes and Vallee in 1957,[1] are a family of small metalloproteins characterized by their high cysteine content, absence of disulfide bonds, and a lack of aromatic amino acids.[2] MT is ubiquitous to living organisms and since its discovery, members of the MT family have been isolated from a wide range of sources including all animal phyla, fungi, plants, as well as cyanobacteria.[3−6] Owing to the significant number of cysteine residues in the sequence (~30% of all amino acids),[7] the function(s) of MT have been postulated to include toxic metal detoxification, protection against oxidative stress and as a metallochaperone involved in the metal ion homeostasis of essential Zn^{2+} and Cu^{+}.[8] However, despite more than 60 years of intense research, the exact *in vivo* roles of MT are still largely unknown.

Mammalian MTs are the most well-studied members of the MT family and consist of 20 cysteine residues that act to encapsulate two metal−thiolate cores. Figure 1A shows a space filling model of human MT 1a coordinated to 7 Cd^{2+} ions, Cd_7-$\beta\alpha$-rhMT 1a (mammalian isoforms other than 1a will be noted specifically). In the X-ray structure of rat liver MT 2 (Zn_2Cd_5-MT 2),[9] and NMR studies from other variants,[10,11] the metal ions exists with two independent domains: an N-terminal β-domain and a C-terminal α-domain. The β-domain is capable of binding 3 Zn^{2+} or Cd^{2+} ions through 9 cysteine residues, while the α-domain is capable of binding 4 Zn^{2+} or Cd^{2+} ions through 11 cysteine residues (Figure 1B). Significantly, the structural data has only been reported from metal-saturated proteins. It is important to note that both Zn^{2+} and Cd^{2+} bind to metallothionein in an isostructural manner, and that the overall molecular architecture of the protein, when coordinated to either Zn^{2+} or Cd^{2+}, is identical.[11] The sequence of the cleaved recombinant $\beta\alpha$-rhMT coordinated to seven divalent metal ions is shown in Figure 1C, with the metal ions colored green and cysteine residues yellow. The numbering of the cadmium-thiolate core is cross referenced to the original naming conventions based on the order of the NMR bands in the mammalian Cd_7-MT 2a spectra,[10] while the numbering of the cysteine residues has been adjusted to accommodate both the additional amino acids from thrombin cleavage (residues 1 and 2) and a series of amino acids meant to aid in protein expression (residues 3−9).

Mammalian MT can be subdivided into 4 distinct subfamilies (MT-1, -2, -3 and -4), each of which contain 20 cysteine residues coordinating 7 divalent metals. However, different patterns of expression suggest specific *in vivo* roles for each subfamily. For example, both MT-1 and -2, found in abundance in the liver and kidneys, are induced by a number of stimuli, including metal ions, glucocorticoids, cytokines and oxidative stress,[3,12,13] while MT-3, found primarily in the central nervous system,[14] and MT-4, found in stratified squamous epithelial tissues, are more tightly controlled.[15] These differences in expression, both causal and spatial, of the MT subfamilies are

Received: December 16, 2011
Published: January 12, 2012

 © 2012 American Chemical Society

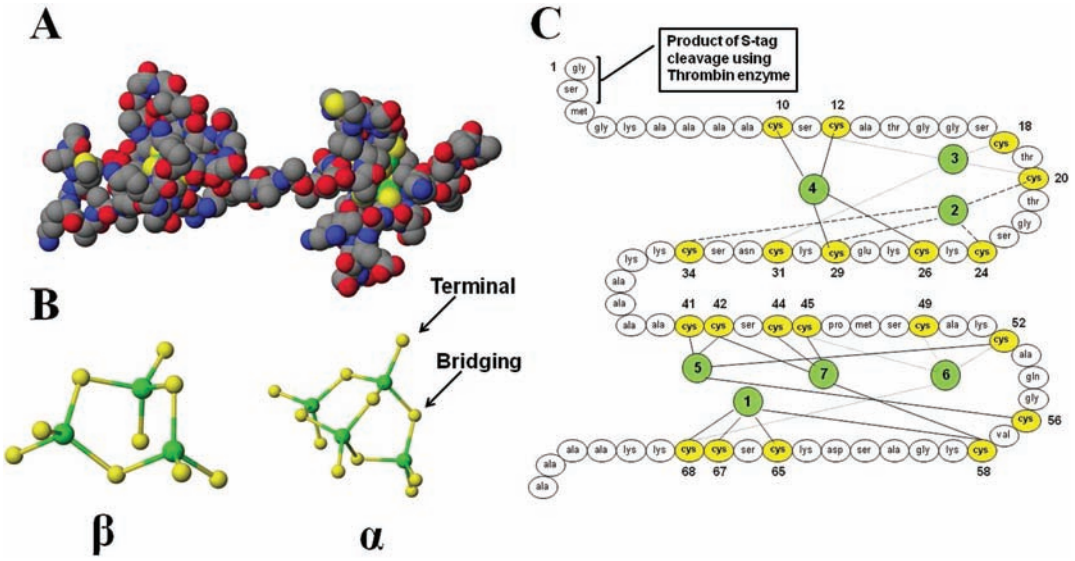

Figure 1. (A) Space filling structure of Cd_7-$\beta\alpha$-rhMT 1a. The N-terminal β-domain is located on the left-hand side, while the C-terminal α-domain is located on the right-hand side. (B) Cadmium-cysteinyl-thiolate clusters of Cd_7-$\beta\alpha$-rhMT 1a presented as a ball and stick model: β-domain (left) and α-domain (right). (C) Connectivity diagram of MT 1a, which shows that each of the seven traditional cadmium atoms is connected to exactly four cysteine amino acids. The connectivity diagram has been renumbered to accommodate the amino acids glycine and serine, both of which are a product of S-tag cleavage with Thrombin, located on the N-terminal of the β-domain. Numbering of the Cd-thiolate centers is based on the NMR assignment by Messerle et al.[10] Molecular modeling data from Chan et al.[22]

likely the result of the unique biological functions of each member. In fact, it has been shown that disruption of the natural expression of MT-3, through ectopic expression in mice, has led to the development of pancreatic acinar cell necrosis and death.[16] These results highlight the fact that a dysregulation in the expression of MT can lead to a diseased state and eventual death. However, little is known regarding the structural differences of these MT subfamilies that must underlie their functional differences.

One reason for the difficulty in determining structure–function relationships for MT is that it is notoriously difficult to crystallize. To date, only two X-ray structures have been reported: the first from rat,[9] Cd_5Zn_2-MT 2, and the second from yeast,[17] Cu_8-MT. In the first case, both cadmium and zinc metal centers were tetrahedrally coordinated by four thiolate groups into two distinct binding domains, while in the second case a combination of both trigonal and diagonal coordination was observed for a single domain Cu-thiolate cluster. Much of the structural information known for mammalian MT is a result of the many NMR-based studies.[10,18−21] While NMR studies can provide the solution structure of MT, analysis has been limited to the spin 1/2 nuclei, namely ^{111}Cd and ^{113}Cd. Unfortunately, because of an absence of interdomain NOEs, NMR studies can only provide the absolute connectivities of atoms in a specific domain and their spatial relationship within that domain's metal–thiolate core. While the X-ray structure of the rat liver Zn_2Cd_5-MT 2 did provide the alignment of the interdomain linkage, the lack of interdomain NOEs has led to the assumption that both domains essentially act independently of each other. Further, subsequent studies have also generally assumed that the metal-based chemistry of each domain must also be independent and significantly that MT will adopt a two-domain structure at all metal loading levels.

The assumption of domain independence has significant consequences for the metal exchange properties of metallothionein. Specifically, the β-domain of MT has been associated with a preference for Cu^+ coordination, while the α-domain has been associated with a preference for Zn^{2+} or Cd^{2+} coordination.[23−25] The question remains, however, if the domains do not interact with one another, then how does the metal binding reaction reach equilibrium? This problem is further complicated by the fact that MT is capable of binding a very wide range of metals, with differing geometries that are dependent on the stoichiometries of the associated metal, for example As_6-MT, Cd_7- or Zn_7-MT, Cu_{12}- or Ag_{12}-MT, and Hg_{18}-MT.[26−29] A recent study with As-MT has shown that As^{3+} distribution between the full protein and the domain fragments occurred by protein–protein interactions, and not by a dissociative-associative mechanism.[30] While not conclusive, these results support the existence of domain–domain interactions as the driving force behind metal–ion equilibration.

Another reason for the difficulty in determining the function of MT is that until recently, MT was thought to coordinate metals in a cooperative fashion, where the binding of one metal facilitates the binding of subsequent metals.[31] However, recent studies have shown that metalation of MT by Cd^{2+}, Zn^{2+}, As^{3+}, and Bi^{3+} occurs in a noncooperative fashion.[26,32−36] A noncooperative mechanism allows for partially metalated, as well as metal exchange intermediates, to be stable and able to take part in cellular chemistry. Significantly, Krezel and Maret have shown from their competition experiments that there exist at least three classes of Zn^{2+} binding site, with log K values of 11.8, ~10 and 7.7 corresponding to the binding of four, two and one metal ion, respectively.[37] This range of binding affinities shows that MT can act as a dynamic metallochaperone, capable of donating and accepting metal ions over a range of cellular concentrations.

Finally, MT has been shown to bind metals in excess of traditional levels. These supermetalated states have been reported for both of the isolated α- and β-domains forming Cd_5-α-rhMT[38] and Cd_4-β-rhMT,[39] respectively. This level of metalation has also been reported in human MT-3, Cd_8-$\beta\alpha$-hMT 3.[40] In the case of MT-1 and MT-2, Cd^{2+} ions are known

dx.doi.org/10.1021/ja211767m | J. Am. Chem. Soc. 2012, 134, 3290−3299

to isomorphously replace Zn^{2+} ions,[41] which suggests the involvement of these supermetalated structures in the metal-exchange reactions that must occur for the binding of incoming metals with binding affinities greater than that of the resident zinc, for example, the essential Cu^{+} and the toxic Cd^{2+}. Indeed, metal transfer reactions in MT have been well documented, for example the Zn^{2+} transfer of fully metalated Zn_7-$\beta\alpha$-MT to m-aconitase,[42] carbonic anhydrase,[43] and the prototypical transcription factor Gal4.[44] Interestingly, a recent study involving the incubation of $A\beta_{1-40}$-Cu^{2+}, a producer of reactive oxygen critical to Alzheimer's disease, with Zn_7-$\beta\alpha$-MT 3 demonstrated that MT readily exchanged Zn^{2+} for Cu^{2+}, with subsequent reduction to Cu^{+} and coordination to the remaining reduced thiols, thereby deactivating the $A\beta_{1-40}$-peptide.[45] While these studies highlight the importance of protein−protein interactions, no exchange intermediates have been characterized that provide insight into the actual mechanism of metal transfer.

In this paper, we present evidence that human metallothionein, Cd_7-$\beta\alpha$-rhMT, is capable of binding an additional cadmium atom to form the structurally unique Cd_8-$\beta\alpha$-rhMT. Exact metal speciation was monitored using ESI-mass spectrometry (ESI-MS), which allowed for a direct correlation between the number of cadmium atoms bound to the protein and observed changes in the UV absorption and CD spectra. Direct and indirect ^{113}Cd NMR spectroscopies were used to ensure that the incoming metal was structurally significant and involved direct interaction with the metal−thiolate cluster. Possible implications of these results with respect to metal ion homeostasis and metal ion domain selectivity are discussed both of which have significant consequences for the *in vivo* function of MT in an organism.

EXPERIMENTAL METHODS

Chemicals. Chemicals used included cadmium sulfate (Fisher Scientific); cadmium(113) chloride (Trace Sciences International Inc.); deuterium oxide (Cambridge Isotopes Laboratories, Inc.); *tris*(2-carboxyethyl)phosphine (PIERCE); ThrombinCleanCleave Kit (Sigma) Tris buffer, tris(hydroxymethyl)aminomethane (EMD Chemicals/VWR); ammonium formate buffer (JT Baker); ammonium hydroxide (Caledon Laboratory Chemicals); formic acid (Caledon Laboratory Chemicals); and hydrochloric acid (Caledon Laboratory Chemicals). All solutions were made with >16 M Ω cm^{-1} deionized water (Barnstead Nanopure Infinity). HiTrap SP HP ion exchange columns (Amersham Biosciences/GE Healthcare), superfine G-25 Sephadex (Amersham Biosciences/GE Healthcare), stirred ultrafiltration cell Model 8010 and 8200 (Amicon Bioseparations/Millipore) with YM-3 membrane (3000 MWCO) were used in the protein purification steps.

Protein Preparation. The expression and purification of recombinant $\beta\alpha$-rhMT has been previously reported.[22] The $\beta\alpha$-rhMT used in this study was based on the 72-residue sequence MGKAAAACSC ATGGSCTCTG SCKCKECKCN SCKKAAAACC SCCPMSCAKC AQGCVCKGAS EKCSCCKKAA AA with no disulfide bonds present in the system. The expression system included, for stability purposes, an N-terminal S-tag (MKETAAAKFE RQHMDSPDLG TLVPRGS). Recombinant $\beta\alpha$-rhMT 1a was expressed in BL21(DE3) *Escherichia coli* transformed using the pET29a plasmid. Removal of the S-tag was performed using a Thrombin CleanCleave Kit. To impede oxidation of the cysteine residues to disulfide bonds, all protein samples were rigorously evacuated and then argon saturated.

CD, UV Absorption Spectroscopic and ESI−MS Spectrometric Measurements. All protein concentrations were confirmed by UV absorption spectroscopy using the absorbance at 250 nm, which corresponds to the ligand-to-metal charge transfer transition generated by the metal−thiolate bond (ε_{250} = 89000 $M^{-1}cm^{-1}$).

CD spectra were recorded on a Jasco J810 spectropolarimeter in a 1 cm quartz cuvette at room temperature (22 °C) using Spectra Manager version 1.52.01 (Jasco). The wavelength range of 200−350 nm was scanned continuously at a rate of 50 nm/min with a bandwidth of 2 nm. The spectral data were organized and plotted using Origin version 7.0383. The CD spectra are expressed in units of ΔA. For the CD titration a solution of Cd_7-$\beta\alpha$-rhMT was prepared in 5 mM ammonium formate (pH 8.1) to a concentration of 7.8 μM. This solution was then titrated in a stepwise manner with increasing amounts of Cd^{2+} using both 0.17 mM and 1.02 mM $CdSO_4$ to produce a solution of Cd_8-$\beta\alpha$-rhMT 1a.

UV absorption spectra were recorded on a Cary 5G UV−vis−NIR spectrophotometer (Varian) in a 1 mm quartz cuvette at room temperature (22 °C) using the Cary Win UV Scan software application. The wavelength range of 200−350 nm was scanned continuously. All spectra were baseline-corrected. The spectral data were organized and plotted using Origin version 7.0383. The sample was measured in a 5 mM ammonium formate buffer at pH 8.1 with a protein concentration of 28 μM. This same sample was used in the ESI−MS titration. The extinction coefficient used for Cd_8-$\beta\alpha$-rhMT 1a was 89000 $M^{-1}cm^{-1}$.

ESI-MS spectra were recorded on a micrOTOF II MS (Bruker). The operating parameters were as follows: End plate offset −500 V; Capillary 4200 V; Nebulizer 2.0 bar; Dry gas 8 L/min; Dry temperature 80 °C; Capillary exit 180 V; Hexapole RF 600 Vpp; Mass range 500−3000 *m*/*z*. Spectra were acquired as a rolling average of 2 × 0.5 Hz. A solution of Cd_7-$\beta\alpha$-rhMT was prepared in 5 mM ammonium formate (pH 8.1) to a concentration of 27.0 μM for MS measurements of Cd_7-$\beta\alpha$-rhMT and Cd_8-$\beta\alpha$-rhMT.

NMR Spectroscopic Measurements. Samples of Cd-bound $\beta\alpha$-rhMT for NMR analysis were prepared by pooling protein product from five 4 L recombinant preparations following thrombin-cleavage of the S-tag. The $^{113}Cd_7$-$\beta\alpha$-rhMT used for acquisition of all NMR spectra was prepared by addition of concentrated formic acid to demetallate the protein, followed by desalting on a G-25 Sephadex column at which point *tris*(2-carboxyethyl)phosphine (TCEP) was added to the solution to impede oxidation. Isotopically pure (>95%) cadmium(113) chloride was added to the solution followed by neutralization using ammonium hydroxide. The solution was then concentrated to 10 mL and desalted into 10 mM ammonium formate buffer using a G-25 Sephadex column at pH 7.5 in order to remove any excess cadmium(113). Concentration, and D_2O exchange to 30% total volume, was performed using Amicon stirred ultrafiltration cell models 8200 and 8010, respectively. The final protein concentration was determined to be 5.3 mM based on UV absorption spectroscopy using the 250-nm peak (ε_{250} = 89000 $M^{-1}cm^{-1}$). The buffer used for this sample was 5 mM ammonium formate (pH 8.3). The sample was Ar-saturated and sealed in a 5 mm NMR tube for analysis. Following acquisition of $^{113}Cd_{7/8}$-$\beta\alpha$-rhMT excess cadmium(113) was added to produce $^{113}Cd_8$-$\beta\alpha$-rhMT, which was used for both the 1D and 2D NMR spectra.

All NMR spectra were acquired on a Varian Inova 600 NMR spectrometer ($\nu_L(^1H)$ = 599.44 MHz, $\nu_L(^{113}Cd)$ = 132.99 MHz) using Varian's VNMRJ 2.2D software with Chempack 3.0 add-on. The ^{113}Cd chemical shifts were referenced with respect to an external 1.0 M solution of $CdSO_4$ in D_2O ($\delta(^{113}Cd)$ = 0.0 ppm), while ^1H chemical shifts were internally referenced to TMS ($\delta(^1H)$ = 0.0 ppm) based on the ^2H frequency of the deuterated solvent.

Direct-detect 1D $^{113}Cd\{^1H\}$ NMR spectra were acquired using a Varian broad-band 5.0 mm HX probe, a spectral range from 540 to 720 ppm, and WALTZ-16 ^1H decoupling during acquisition only. For $Cd_{7/8}$-$\beta\alpha$-rhMT 1a, a total of 39000 transients were accumulated, while Cd_8-$\beta\alpha$-rhMT 1a had a total of 30176 transients accumulated. Both used a 7 s relaxation delay and a 5.33 μs 60-degree pulse width with a 0.684 s acquisition time at room temperature. The data were processed using a line-broadening of 10 Hz.

Indirect 2D ^1H−^{113}Cd HSQC NMR spectra were acquired using a Varian indirect-detection 5.0 mm HCX probe, a ^{113}Cd spectral range from 540 to 720 ppm, a ^1H spectral range from −0.5 to 10 ppm, a 0.291 s acquisition time, and a 2 s relaxation delay. Water suppression

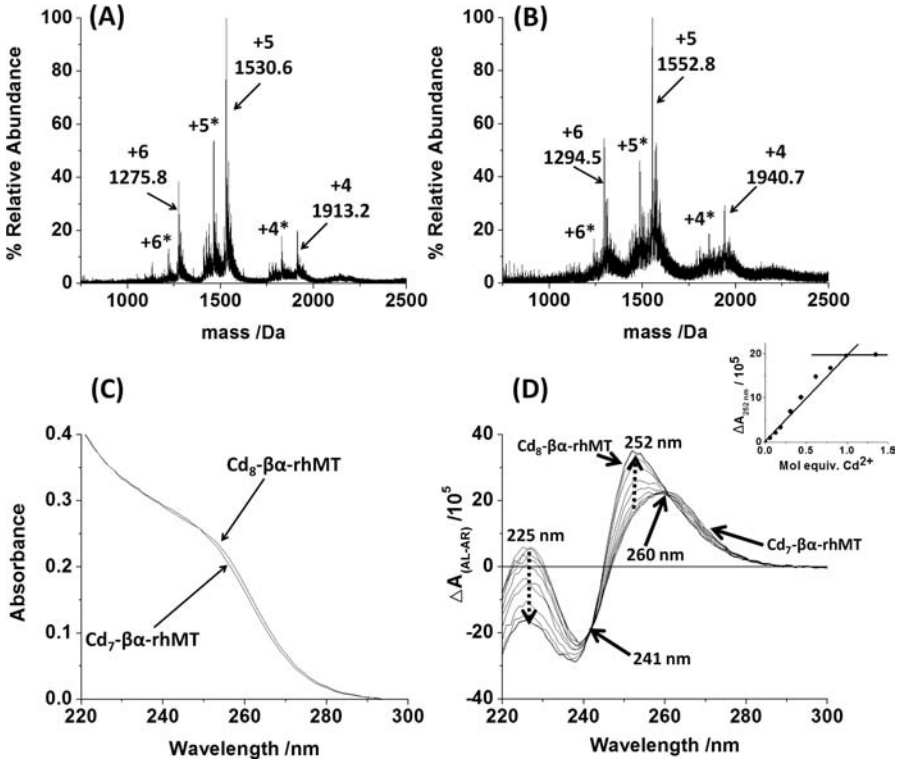

Figure 2. ESI-MS spectra of (A) Cd_7-$\beta\alpha$-rhMT and (B) Cd_8-$\beta\alpha$-rhMT with 0.0 and 2.8 excess molar equivalents of $CdSO_4$, respectively. The charge states marked with an asterisk(*) are the result of a small fraction of truncated protein. (C) UV absorption spectra of Cd_7-$\beta\alpha$-rhMT and Cd_8-$\beta\alpha$-rhMT with 0.0 and 2.8 excess molar equivalents of $CdSO_4$, respectively. (D) CD spectral changes observed during the incremental titration of Cd_7-$\beta\alpha$-rhMT with $CdSO_4$ to form Cd_8-$\beta\alpha$-rhMT. Aliquots of $CdSO_4$ were added to solution in mole equivalents (based on the whole protein) of 0.00, 0.03, 0.06, 0.13, 0.19, 0.44, 0.62, 0.80, 0.99, and 1.35. The inset in (D) shows the change in absorbance at 252 nm as a function of Cd^{2+} added to solution. Past the addition of one molar equivalent Cd^{2+}, there is no change in the CD spectrum.

was achieved using a selective 2 s presaturation pulse at a power of 13 dB. In the indirect ^{113}Cd dimension the data was zero-filled to 1024 total points, and a Gaussian weighting function was applied. In the direct ^1H dimension, the data were zero-filled to 1024 points and a Gaussian weighting function was applied. For both $Cd_{7/8}$-$\beta\alpha$-rhMT 1a and Cd_8-$\beta\alpha$-rhMT 1a, a total of 80 transients were accumulated for each of the 128 increments, a forward linear prediction of 128 points in ^{113}Cd dimension, and the $^3J(^{113}Cd,^1H)$ value was set to 67 Hz at room temperature.

Molecular Model. MM3/MD calculations parametrized using the modified force field described by Chan et al.[46] and the dielectric constant for water (78.4) were carried out to obtain the minimum-energy structure of Cd_8-$\beta\alpha$-rhMT 1a. All MM3/MD calculations and model-structure rendering were carried out using CAChe WorkSystem Pro 6.1.1 Software (Fujitsu America). The original Cd_7-$\beta\alpha$-rhMT 1a was modified using CAChe to produce molecular models for Cd_8-$\beta\alpha$-rhMT 1a.[22] The structure was energy-minimized as follows: (1) the structure was energy minimized using the MM3 calculation followed by the MD simulation at 500 K for 1000 ps and (2) the lowest structure was taken and again minimized at 300 K for 5000 ps.

RESULTS

Supermetalation of $\beta\alpha$-rhMT with Cd^{2+} Monitored by ESI-Mass Spectrometry and CD and UV Absorption Spectroscopies. To determine the effect of the eighth metal on the overall fold of the protein, analysis with both CD and UV absorption spectroscopy, coupled with metal speciation provided by ESI-MS, were used. These techniques correlate the number of metals bound to the observed spectroscopic changes in solution. The protein used in these experiments was taken directly after purification and desalted into an ESI-MS compatible buffer. This was carried out to avoid structural changes that may occur upon acid induced demetalation and to demonstrate that the additional low affinity site for Cd^{2+} is not the result of high concentrations found in the NMR experiment.[47]

A solution of Cd_7-$\beta\alpha$-rhMT (Figure 2A) was initially measured. Addition of 2.8 excess molar equivalents of Cd^{2+} quantitatively converted Cd_7-$\beta\alpha$-rhMT to Cd_8-$\beta\alpha$-rhMT (Figure 2B). In the MS spectra, two sets of truncated $\beta\alpha$-rhMT were detected: one in which the N-terminal G residue and C-terminal AA residues were truncated, and a second in which the N-terminal GSMGK as well as A from either the N-terminal or C-terminal were truncated. None of the metal-binding cysteine residues were affected. This truncation has been previously reported, and it does not affect the metal binding properties of the protein.[32] The former truncation is of greater intensity and was used for all metal binding analyses. The theoretical m/z values of Cd_7-$\beta\alpha$-rhMT are 1275.5 m/z for +6, 1530.4 m/z for +5 and 1912.7 m/z for +4, while the theoretical mass is 7647 Da. These theoretical data are essentially identical to the experimental results of 1275.8 m/z for +6, 1530.6 m/z for +5 and 1913.2 m/z for +4 and a mass of 7649 Da. The theoretical m/z values of Cd_8-$\beta\alpha$-rhMT are 1293.9 m/z for +6, 1552.5 m/z for +5 and 1940.4 m/z for +4, while the theoretical mass is 7,757 Da. These theoretical values also compare well with the experimental results of 1294.5 m/z for +6, 1552.8 m/z for +5 and 1940.7 m/z for +4 and a mass of 7759 Da. Of significance, is that the conversion of Cd_7-$\beta\alpha$-rhMT into Cd_8-$\beta\alpha$-rhMT leads to an increase in the relative intensity of the +6 charge state from 38% to 55% and a decrease in the absolute intensity of the +5 charge state. These

changes in intensity may be attributed to an increase in the overall volume of the protein necessary to accommodate the binding the eighth Cd^{2+} ion.[48,49]

The effect of the addition of the eighth cadmium ion was also analyzed using both UV absorption and CD spectroscopy to determine the effects of this additional ion on the metal–thiolate cores. The UV absorption spectrum did not change significantly upon formation of Cd_8-$\beta\alpha$-rhMT (Figure 2C). This was observed previously for the formation of the supermetalated Cd_4-β-rhMT and Cd_5-α-rhMT.[38,39] The lack of change in the UV absorption profile with the addition of an eighth Cd^{2+} ion is likely related to the necessity for the formation of only bridging interactions, and no new terminal interactions.

Addition of 1 mol equiv Cd^{2+} led to significant changes in the CD spectrum (Figure 2D). The original maxima and minima of 260 and 239 nm observed for Cd_7-$\beta\alpha$-rhMT were replaced by maxima and minima of 252 and 238 nm, respectively. Significant reduction in the intensity of the maxima located at 225 nm was also observed. Two isodichroic points are observed throughout the titration at 260 and 241 nm and provide evidence for the direct conversion of Cd_7-$\beta\alpha$-rhMT to Cd_8-$\beta\alpha$-rhMT. For Cd_7-$\beta\alpha$-rhMT the maximum at 260 nm was broad suggesting that the traditional structure is flexible and exists as a mixture of conformations. However, upon supermetalation of Cd_7-$\beta\alpha$-rhMT to form Cd_8-$\beta\alpha$-rhMT the maximum blue-shifted to 252 nm and the intensity increased by 50%. The increase in intensity may be attributed to a decrease in the conformational flexibility of the protein, while the blue shift can be associated with the metal ion directly interacting with the metal–thiolate core. These changes to the CD envelope provide strong evidence that the eighth Cd^{2+} atom coordinates to both the β- and α-domain.

The inset in the CD titration (Figure 2D) shows that no change in the absorbance at 252 nm is observed after a single molar equivalent of Cd^{2+} has been added to solution of Cd_7-$\beta\alpha$-rhMT. We interpret the maxima at 252 nm to be exclusively the result of the Cd_8-$\beta\alpha$-rhMT species. Cd_7-$\beta\alpha$-rhMT binds the additional Cd^{2+} ion with a significantly greater affinity than either Cd_3-β-rhMT or Cd_4-α-rhMT bind the additional Cd^{2+} to form their respective supermetalated species.[38,39]

One dimensional ^{113}Cd NMR spectroscopy of both Cd_7-$\beta\alpha$-rhMT and Cd_8-$\beta\alpha$-rhMT. Direct 1D $^{113}Cd[^1H]$ NMR spectra were measured for a mixture of $Cd_{7/8}$-$\beta\alpha$-rhMT, a result of a slight excess of Cd^{2+} to increase resistance to oxidation, and a pure sample of Cd_8-$\beta\alpha$-rhMT in order to determine the relative speciation of the individual metal binding sites as well as the type of coordinating ligands through chemical shift data. In the $Cd_{7/8}$-$\beta\alpha$-rhMT spectrum, peaks 1, 5, 5′, 6 and 7 correspond to the α-domain, while peaks 2, 3, and 4 correspond to the β-domain.[50] Signals observed for $Cd_{7/8}$-$\beta\alpha$-rhMT (Figure 3A) include resonances at 673, 668, 650, 647, 631, 629, and 621 ppm, where the resonances at 673, 631, 629, and 621 ppm result from the α-domain and 668, 650, and 647 ppm result from the β-domain. An additional peak labeled(*) located at 680 ppm has been previously observed and is likely the result of the presence of some metal-based heterogeneity in the Cd_7-$\beta\alpha$-rhMT sample. This assignment is based, in part, on previous NMR work of human liver Cd-MT 1 by Boulanger and Armitage.[50] The observed signals for the pure Cd_8-$\beta\alpha$-rhMT (Figure 3B) are 690, 647, 637, and 595 ppm. The chemical shift range of all the peaks is between 590 and 700 ppm, which overlaps significantly with the region expected for

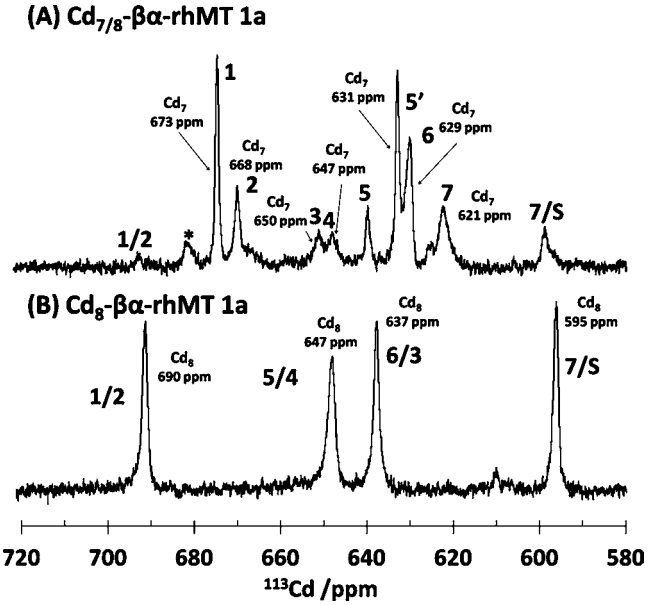

Figure 3. Direct 1D $^{113}Cd[^1H]$ NMR spectrum (133 MHz) of (A) a mixture of Cd_7-$\beta\alpha$-rhMT and Cd_8-$\beta\alpha$-rhMT and (B) Cd_8-$\beta\alpha$-rhMT formed by addition of excess $^{113}CdCl_2$. The $Cd_{7/8}$-$\beta\alpha$-rhMT was prepared in 5 mM ammonium formate pH 8.3 and buffer exchanged into 30% D_2O. Because of the slight excess of $^{113}Cd^{2+}$, a portion of the sample has been converted to Cd_8-$\beta\alpha$-rhMT leading to the formation of additional peaks at 692 and 595 ppm. Subsequent addition of crystalline $^{113}CdCl_2$ to $Cd_{7/8}$-$\beta\alpha$-rhMT led to the formation of Cd_8-$\beta\alpha$-rhMT, which greatly simplifies the spectra reducing it to 4 peaks. Spectra of $Cd_{7/8}$-β-rhMT and Cd_8-β-rhMT were acquired at room temperature.

tetrahedral cadmium-thiolate clusters.[51] A region commonly found for the NMR spectra of Cd-metallothioneins, as well as both trigonal cadmium thiolate and tetrahedral cadmium-thiolate clusters where a single sulfur has been replaced by water, or opportunistic chloride ion.[52] No signals in the range of 200–250 nm were observed, which had been previously observed for supermetalated Cd_5-α-rhMT.[38]

Direct detection of ^{113}Cd in the binding site allows one to infer the fluctionality of the individual metal sites. Analysis of the spectrum in Figure 3A shows that resonances attributed to the β-cluster are significantly less intense than those attributed to the α-cluster. Previous NMR studies involving both domains have shown the α-domain is less fluctional than the β domain leading to sharper peaks of greater intensity for the α-domain.[50] Addition of excess $^{113}Cd^{2+}$ eliminates the spectral complexity associated with the two isolated domains. The loss of all seven unique Cd^{2+} signals associated with the Cd_7-MT and the formation of four unique peaks strongly suggests that the addition of the singular Cd^{2+} to Cd_7-$\beta\alpha$-rhMT leads to the loss of the isolated clusters in favor of a coalesced, single domain of a "super cluster". While all four peaks are of similar size and intensity, the signal located at 647 ppm is slightly broader and less intense. This suggests that the metal-ion associated with this binding site is more solvent exposed and fluctional. Consequently, it is likely that this smaller broader peak is the most likely candidate for the site of metal loss in the metal-exchange intermediate, allowing both the solvent and acceptor/donor proteins access to the metal-ion. The sharpness of the spectral lines further supports the interpretation of CD spectroscopic data that the maxima blue shift between Cd_7-$\beta\alpha$-rhMT and Cd_8-$\beta\alpha$-rhMT, with an increase in intensity of

dx.doi.org/10.1021/ja211767m | J. Am. Chem. Soc. 2012, 134, 3290–3299

50%, is the result of a reduction in the fluctionality of the protein.

Two Dimensional $^{1}H[^{113}Cd]$ HSQC NMR Spectroscopy of Both Cd_7-$\beta\alpha$-rhMT and Cd_8-$\beta\alpha$-rhMT. Indirect ^{1}H-$[^{113}Cd]$ HSQC NMR spectra were measured for both Cd_7-$\beta\alpha$-rhMT and Cd_8-$\beta\alpha$-rhMT (Figure 4). Analysis of the β protons

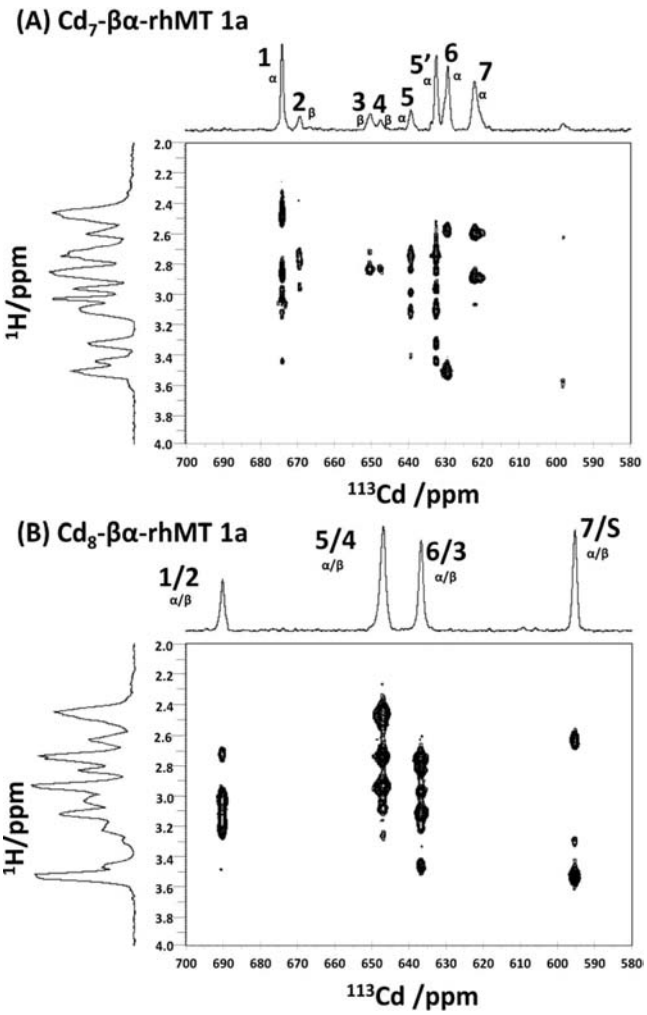

Figure 4. Indirect 2D $^{1}H[^{113}Cd]$ HSQC NMR of (A) Cd_7-$\beta\alpha$-rhMT 1a and (B) Cd_8-$\beta\alpha$-rhMT 1a formed by addition of excess $^{113}CdCl_2$. While a total of eight peaks exist for Cd_7-$\beta\alpha$-rhMT, it can be clearly seen that 5 and 5′ have similar proton profiles. This heterogeneity has been previously reported by Boulanger and Armitage[50] and is attributed to a slight difference in two structural conformers of the protein. The signals in (B) are the labeled based upon the assignments of the isolated Cd_4-β-rhMT and Cd_5-α-rhMT.[38,39] The peak labeled 7/S is what we consider to be the site of supermetalation and we believe that this may represent a tetrahedral geometry coordinating either four thiolates or three thiolates and a single water molecule/chloride ion.

of the cysteine residues allowed determination of peak relatedness. Peaks were interpreted as related based on similarity in both the ^{1}H and ^{113}Cd chemical shifts. In the case of Cd_7-$\beta\alpha$-rhMT (Figure 4A), both signals 1 and 2 have the same overall profile as those of the isolated domains, and are attributed to the α- and β-domain, respectively. Signals 3 and 4 result from the remaining two cadmium ions found in the β-domain and are significantly downfield compared to their counterparts found in the isolated domains (isolated β-domain 630 and 616 ppm compared with the full protein 650 and 647 ppm).[39] We interpret this difference as the result of the effect of the α-domain on the chemical shifts of the β-domain. Signals 5 and 5′ are both attributed to the same cadmium atom found in the α-domain and have a similar cysteine β proton profile. Signals 6 and 7 both correspond to α-domain and have similar chemical shifts to those of the isolated α-domain (isolated α-domain 626 and 611 ppm compared with the full protein 629 and 621 ppm).[38]

The loss of cluster identity when Cd_7- is converted into Cd_8-$\beta\alpha$-rhMT (Figure 4B) significantly simplifies the spectra and the addition of the eighth metal ion results in dramatic changes to the β proton profile of all peaks. These changes indicate that there are significant structural rearrangements taking place to accommodate all metal ions. Interestingly, no signal was observed in the 245−215 ppm region that had previously been assigned to the supermetalated $Cd(RS)_2(OH_2)_4$ of the α-domain. This suggests that the supermetalated cadmium ion found in Cd_8-$\beta\alpha$-rhMT is directly coordinated to at least 3 cysteine residues. With the exception of the previously mentioned $Cd(RS)_2(OH_2)_4$, the previously reported ^{113}Cd NMR data for the supermetalated isolated domains, have exactly four $^{113}Cd^{2+}$ signals located between 700 and 600 ppm. and the tentative assignment of peak identity for the Cd_8-rhMT 1 was based upon this similarity.[38,39]

Note that supermetalation of the β-domain leads to an inversion of the location of the 3 and 4 peak, such that 4 is found further downfield than 3. The β proton profile of Cd_8-$\beta\alpha$-rhMT is somewhat more complex than either isolated domain, indicating overlap of the profiles of both domains. It should be noted at this time that there are two reasons why we have not assigned a specific cysteine residue to each 2-D signal: the first is that signals associated with the β-domain are significantly less intense than those associated with the α-domain and their overlap further complicates the spectra, the second reason is that in order to conclusively assign the identity of the peaks, one would require a complete backbone assignment. This type of assignment has been not been carried out yet for human MT-1a.

Figure 5 provides a graphical comparison of the NMR data for MT isoforms 1−3, as well as the supermetalated data for both Cd-MT and its isolated domains. The value of this Figure is that it shows the NMR range where MT-cadmium-thiolate clusters are found. The presence of the eighth cadmium atom causes both the β- and α-domains to adopt supermetalated character. This is strong evidence that this eighth cadmium atom is coordinated to Cys previously in both domains. Also important to this Figure is the observation that all NMR peaks, with the exception of supermetalated Cd_5-α-rhMT, fall between 700 and 590 ppm. It can be clearly seen that Cd_8-$\beta\alpha$-rhMT, Cd_5-α-rhMT and Cd_4-β-rhMT all exhibit nearly identical ^{113}Cd signals in the 700−590 ppm range. This was a surprising result since it had been previously thought that supermetalation of the full protein would lead to either 9 unique signals, indicative of Cd_9-$\beta\alpha$-rhMT 1a, or alternatively would only alter the metal binding sites of one of the two domains. We interpret this overlap to mean that supermetalation of the isolated domains is in fact the result of residual metal binding capacity. This is supported by CD titrations of all three, where the isolated β- and α-domains require an excess of Cd^{2+} to supermetalate and the full protein is completely supermetalated at exactly 1 equivalent (Figure 2). Consequently, we propose based on these experimental results, that Cd_8-$\beta\alpha$-rhMT 1a adopts a new

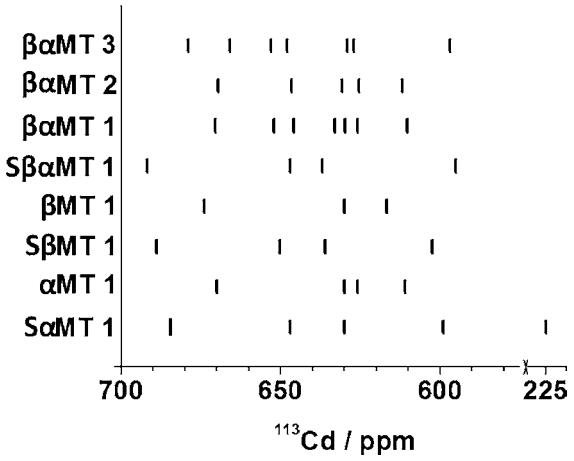

Figure 5. Comparison of the ^{113}Cd NMR resonances for the human MTs: Cd_7-$\beta\alpha$-MT 3,[21] Cd_7-$\beta\alpha$-MT 2,[50] Cd_7-$\beta\alpha$-MT 1a,[50] supermetalated Cd_8-$\beta\alpha$-rhMT 1a (this work), Cd_3-β-rhMT 1a,[39] supermetalated Cd_4-β-rhMT 1a,[39] Cd_4-α-rhMT 1a[38] and supermetalated Cd_5-α-rhMT 1a.[38] Note the significant overlap in the location of signals associated with both isolated domains of MT and the full protein. The sole exception to this similarity is the presence of a single peak at 224 ppm associated with supermetalated Cd_5-α-rhMT, which is both absent from supermetalated Cd_4-β-rhMT and supermetalated Cd_8-$\beta\alpha$-rhMT.

MT structural motif that requires the coalescence of both domains to a single binding domain.

DISCUSSION

For the last sixty years, MT has been proposed to be involved in metal homeostasis, toxic metal detoxification and in the protection of organisms against oxidative stress.[8] And while it is likely that MT is involved in all three of these processes, the exact cellular function(s) have never been determined. Critical to these roles are MT's ability to act as a metallochaperone capable of coordinating incoming metal ions and exchanging them with the cellular environment. Indeed several studies have demonstrated the importance of MT in both donating to and accepting metal ions from other metalloproteins.[42−44] These studies have highlighted the importance of protein−protein interactions, but a metal-exchange intermediate has not been observed. Several studies have documented the preference of the β-domain for Cu^+ ions and the α-domain for Zn^{2+}/ Cd^{2+} ions.[23,45,53] Since Zn^{2+} coordination dominates mammalian MT,[54] an incoming metal of higher binding affinity (Cd^{2+} or Cu^+) must either (1) coordinate in a domain specific manner or (2) coordinate through either domain with a subsequent redistribution of metals leading to the observed metal-domain preferences. Copper luminescent studies of MT have provided evidence for a fluctional model of the protein, in which initial metalation occurs in a distributed manner, statistically across both domains, followed by a rearrangement of both clusters to their lowest energy conformers.[25,28] However, this model would require an intraprotein intermediate, in which both domains exchange metals with each other. To date both the β- and α-domains of fully metalated MT are considered isolated, because of both a lack of interdomain NOEs and the independence of their respective ^{113}Cd signals in NMR studies.[10,20,55]

We report here, for the first time, conclusive evidence for the presence of domain−domain interactions in fully metalated MT from experimental observation of a species in which one Cd^{2+} is proposed to bridge both domains. Formation of Cd_8-MT species results in the loss of specific α and β domain character and the formation of a single, Cd_8Cys_{20} domain. This supermetalated species provides evidence for the type of intermediate that is critically important in the metal exchange pathway necessary for the observed domain selectivity of metal ions. Implicit in this structure is the existence of a "super domain", where both domains contribute cysteine residues to produce a single Cd_8Cys_{20} cluster in MT 1a. This supermetalated structure has been effectively "frozen" by the higher binding constant of Cd^{2+}, compared with Zn^{2+}, and is likely critical in the metal exchange reactions necessary for MT's role as a metallochaperone.

Initial ESI-MS studies of the apoprotein of MT provided the first evidence that the Cd_7-$\beta\alpha$-rhMT species was able to supermetalate to form Cd_8-$\beta\alpha$-rhMT.[32] However, prior to this report it was unclear whether this additional metal was bound to either metal−thiolate core found in the protein, or if the eighth Cd^{2+} was somehow bound to other ligands. The coupling of both spectroscopic and spectrometric analyses (Figure 2) demonstrates that the addition of only a single equivalent of Cd^{2+} to the fully metalated Cd_7-rhMT protein causes structural changes, which lead to a significant change in the symmetry of the eight Cd^{2+} ions bound in the cluster. This rearrangement breaks the symmetry of both original clusters, observed from the simultaneous loss of exciton coupling in the CD spectrum, but with little change in the ligand-to-metal charge transfer profile. ESI-MS spectral data also show that only a single Cd^{2+} ion is found to coordinate to the protein, and further that this additional metal ion causes an increase in the relative intensity of the +6 charge state compared with the +5 charge state. This suggests that the protein must adopt a significantly larger structure to accommodate the additional metal ion. The observation of two simultaneous isodichroic points during the CD titration of Cd_7-$\beta\alpha$-rhMT with Cd^{2+} is evidence for the direct conversion of Cd_7-$\beta\alpha$-rhMT to Cd_8-$\beta\alpha$-rhMT with no intermediate structures (Figure 2D). The location of the ^{113}Cd-NMR chemical shifts demonstrate conclusively that the additional metal directly interacts with the metal−thiolate core and that this metal ion greatly simplifies the seven unique Cd^{2+} sites to four unique Cd^{2+} sites. Taken together these results demonstrate that supermetalation of MT 1a with Cd^{2+} leads solely to the formation a bridged Cd_8Cys_{20} structure as the final product of metalation.

Based on the previous stoichiometric data for the isolated supermetalated domains of Cd_4-β-MT and Cd_5-α-MT it would be reasonable to predict that the supermetalated full protein would involve 9 Cd^{2+} ions. However, only Cd_8-MT was actually formed. This now allows us to propose that the two-domain structure does not exist generally for all metal loadings, rather only for specific metal loadings. For Zn^{2+} and Cd^{2+} this would occur at 7 metals per MT protein.

In addition to Cd-hMT-1a, Cd-hMT-3 has also been confirmed to supermetalate by 1-D ^{113}Cd NMR spectroscopy.[40] Cd-hMT-3 is primarily found in the central nervous system and, unlike MT-1a and -2, its expression is strictly controlled.[12,13] In the central nervous system MT-3 is thought to control metal ion homeostasis and has been shown to be down-regulated in some Alzheimer's patients.[14] Unlike Cd-hMT-1a, the supermetalated NMR spectra of Cd-hMT-3 does not simplify to four peaks. Moreover, the CD spectrum of MT-3 does not exhibit a loss of exciton coupling found in the

supermetalation of MT-1a. However, the formation of supermetalated Cd-hMT-3 does result in a decrease in the Stoke's radius of this protein, which suggests the mutual approach of the two domains. We should note, that neither Meloni et al. studying Zn_7-MT-2 using both spectroscopic and spectrometric techniques,[40] nor Stillman et al. studying rabbit liver Cd_7MT 2a by CD spectroscopy[56] found that MT-2 was capable of supermetalation. These differences between isoforms may be critical to the cellular role of each MT isoform. It is probable that supermetalated structures of Cd-hMT-1s and -3 are different. On the basis of these observations, we postulate that the ability of a particular MT isoform to supermetalate and the subsequent structure formed from this process are factors that lead to the differentiation of each isoform (MT-1a,-2,-3 and -4) into specific functions in cellular chemistry.

This metal exchange structure could have significant consequences for both the metal ion homeostasis and toxic metal detoxification properties of an organism. Previous studies, using CD, UV and NMR spectroscopies have shown that Cd^{2+} binding to both apo-MT or Zn_7-MT leads to the formation of Cd_7-MT with almost identical absorption and CD properties.[23,56,57] These experiments suggest that regardless of initial status of the MT, it is capable of assuming the same conformation when fully metalated. When the protein is fully metalated, such as Zn_7-MT, the incoming metal ion must be able to coordinate and expel a previously bound Zn^{2+}. In the case of Zn_7-MT, the formation of a transient M_1Zn_7-$\beta\alpha$-rhMT 1a can be envisioned as an exogenous Cd^{2+}, or Cu^{+}, ion coordinating to Zn_7-$\beta\alpha$-rhMT 1a, bridging both domains with subsequent rearrangement and expulsion of a previously bound Zn^{2+} ion. The net effect would be (1) metal ion selectivity (for example, Cu^{+} in the β-domain and Zn^{2+}/Cd^{2+} in the α-domain) and (2) up-regulation of metallothionein allowing an organism to effectively combat toxic metal exposure. A regulator of metallothionein transcription, the metal-responsive-element-binding transcription factor-1 (MTF-1), has been shown to up-regulate metallothionein upon binding to Zn^{2+} ions.[58,59] MTF-1 has been implicated in cellular responses including toxic metal detoxification and oxidative stress, both of which are implicated functions of metallothionein. The metal binding site of this transcription factor includes six Cys_2His_2 zinc fingers, making it exceptionally sensitive to an organism's zinc load. Cell free transcription experiments have shown a number of stresses, including exposure to Cd^{2+}, Cu^{+} and H_2O_2 function by displacing naturally bound Zn^{2+} from MT.[60] These free Zn^{2+} ions bind to MTF-1 leading to a translocation of MTF-1 from the cytoplasm to the nucleus where the Zn-MTF-1 interacts with metal response elements (MREs) leading to up-regulation of MT. In this way, MT is capable of countering and deactivating a wide range of insults to return an organism to homeostatic balance.

For this reason, supermetalation, in the context of toxic metals, may be a critical transient species in the regulation of transcription of the protein. An incoming toxic metal, such as Cd^{2+}, could coordinate in a supermetalated position allowing both sequestration of the toxic metal and release of a Zn^{2+} ion. This Zn^{2+} ion would consequently lead to the up-regulation of MT, through the Zn^{2+} binding motifs of MTF-1, allowing an organism to effectively combat toxic metals. Through this mechanism, supermetalation of metallothionein, the organism would be able to control the cellular metal load.

Surprisingly, we did not observe any evidence for the existence of a Cd_9-$\beta\alpha$-rhMT species, which had previously been suggested to exist based on the summation of the metalation status of the individual supermetalated β- and α-domains. These observed supermetalated states, Cd_4-β-rhMT and Cd_5-α-rhMT, are likely the result of the residual metal binding capacity necessary for both domains to work in concert to form Cd_8-$\beta\alpha$-rhMT. Unlike other metalation studies, which reported the collapse of the two domain structure, for example Hg- and Ag-MT, supermetalation to Cd_8-$\beta\alpha$-rhMT does not require a change in coordination number of the metal ion.[29,61,62]

We have calculated a tentative model based on all eight Cd^{2+} ions being tetrahedrally coordinated to four cysteine residues, which leads to a complete collapse of the two-domain structure (Figure 6A). While qualitative in nature, the structure presented shows how the addition of the eighth Cd^{2+} ion leads to the complete loss of cluster identity (Figure 6B). Through supermetalation, the bridging of both domains provides the intraprotein interactions necessary for metal ion selectivity. The coordination of the eighth Cd^{2+} ion in this model accounts for the absorption, CD and NMR spectral data of Cd_8-$\beta\alpha$-rhMT. In the case of the CD titration, supermetalation of MT essentially locks the two domains in place resulting in a loss of conformational freedom and explains increased sharpness of the Cd_8-MT spectra. In the case of the NMR spectra, the complete collapse of the Cd_7-MT spectra is the result of loss of cluster identity upon binding of the eighth Cd^{2+} ion.

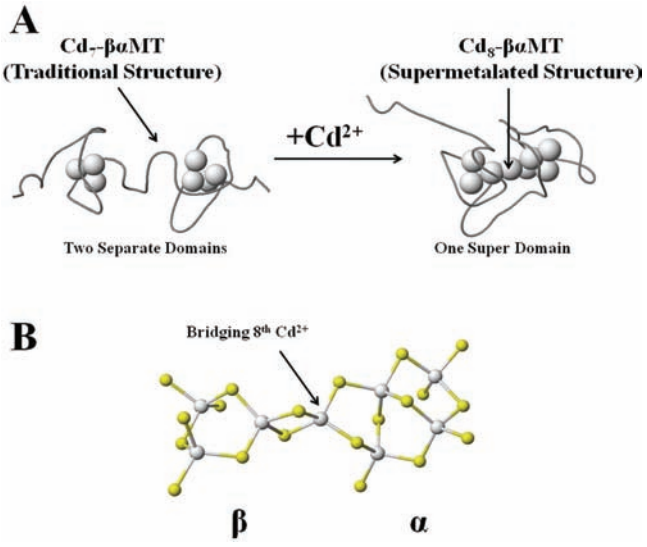

Figure 6. Molecular model of a possible structure for the supermetalated Cd_8-$\beta\alpha$-rhMT 1a structure. (A) Ribbon structure of the backbone of Cd_7-$\beta\alpha$-rhMT and Cd_8-$\beta\alpha$-rhMT with the cadmium atoms represented as spheres calculated using a locally modified force-field with MM3/MD methods for molecular modeling.[46] The N-terminal β domain is located on the left-hand side, while the C-terminal α domain is located on the right-hand side. (B) Cadmium-cysteinyl-thiolate clusters of Cd_8-$\beta\alpha$-rhMT 1a are presented as a ball-and-stick model: β domain (left) and α domain (right). The structure was created by inserting an additional Cd^{2+} ion between the two domains, and minimizing the structure in two steps: (1) 1000 ps at 500 K and (2) 5000 ps at 300 K. The conformer with the lowest energy is presented above. The initial structure of the Cd_7-$\beta\alpha$-rhMT 1a was provided by Chan et al.[22]

Much current research on MT include its interaction with metal based anticancer drugs, such as cisplatin.[63] In these cases, MT has been implicated as a cause for the development of

dx.doi.org/10.1021/ja211767m | J. Am. Chem. Soc. 2012, 134, 3290−3299

cisplatin resistant cancers.[64−66] Karotki and Vasak have found that the binding of Pt^{2+} to MT occurs via a two step reaction and further that the β-domain is the preferred site of coordination. In the context of supermetalation, initial coordination likely leads to a coalescence of both domains with subsequent ejection of one of the previously bound metals of the β-domain.[67] These researchers have also characterized a previously unknown DNA-*cis*-Pt-MT ternary structure, where coordination of the DNA bound cisplatin does not lead to the release of significant Zn^{2+} in Zn_7-MT. These results suggest that coordination occurs in a site specific manner through two sets of solvent exposed cysteine residues found in the β- and α-domain.[68] The role of supermetalation in the initial coordination of metal-based chemotherapeutics may be of significant importance for the development of future chemotherapeutics.

It is now becoming evident that MT has a significant role in the body's response to neuroinflammation.[69] Recently, a report by Manso et al. has demonstrated that the full MT-1 was able to improve the performance of MT knockout mice whose cortex had been damaged through cryoinjury.[70] Most interestingly, the authors report that exposure of the mice to the isolated MT fragments, β and α, result in markedly different recovery rates compared to the full $\beta\alpha$-protein. While the exact mechanism of action is not known, it could be postulated that supermetalation of the full protein, which has significantly greater affinity than either of the two isolated domains, is the causative agent in recovery. Thus full MT acts as a superior metallochaperone when compared to the isolated domains.

CONCLUSION

In summary, the collapse in the number of unique ^{113}Cd-NMR peaks from seven to four, the significant changes in the CD spectral envelope and the quantitative formation of Cd_8-$\beta\alpha$-rhMT and not Cd_9-$\beta\alpha$-rhMT are paradigm shifting with respect to the structural motifs in metallothioneins. The spectroscopic evidence reported in this paper indicate that the β- and α-clusters act in isolation under only very specific metalation conditions. The supermetalated Cd_8-rhMT 1a protein adopts a novel single domain structure suggesting that the well-known two-domain structure might be the special case in the metal-dependent structural landscape of MTs. Further, with these results we are now able to account for both the ability of MT to exchange metals with the solution and the observed metal ion selectivity of the individual domains.

AUTHOR INFORMATION

Corresponding Author

*martin.stillman@uwo.ca

Notes

The authors declare no competing financial interest.

ACKNOWLEDGMENTS

We thank NSERC of Canada for financial support through a Discovery Grant and a Research Tools and Instruments Grant, and through an Academic Development Fund Grant from The University of Western Ontario (to M.J.S.), and an Alexander Graham Bell Canada Graduate Scholarship (CGS) (to D.E.K.S.). We thank Mr Doug Hairsine for technical assistance.

ABBREVIATIONS

MT, metallothionein; β-rhMT, recombinantly prepared beta domain of human metallothionein isoform 1a; α-rhMT, recombinantly prepared alpha domain of human metallothionein isoform 1a; $\beta\alpha$-rhMT, recombinantly prepared human metallothionein isoform 1a; HSQC, heteronuclear single quantum coherence; ESI, electrospray ionization; MS, mass spectrometry; CD, circular dichroism.

REFERENCES

(1) Margoshes, M.; Vallee, B. L. *J. Am. Chem. Soc.* **1957**, *79*, 4813.
(2) Kojima, Y. In *Methods in Enzymology: Metallobiochemistry Part B Metallothionein and Related Molecules*; Riordan, J. F., Vallee, B. L., Eds.; Academic Press, Inc.: San Diego, 1991; Vol. *205*, p 8.
(3) Kagi, J. H. R. In *Metallothionein III: Biological Roles and Medical Implications*; Suzuki, K. T., Imura, N., Kimura, M., Eds.; Birkhauser Verlag: Basel, 1993; p 29.
(4) Blindauer, C. A.; Harrison, M. D.; Parkinson, J. A.; Robinson, A. K.; Cavet, J. S.; Robinson, N. J.; Sadler, P. J. *Proc. Natl. Acad. Sci. U.S.A.* **2001**, *98*, 9593.
(5) Freisinger, E. *J. Biol. Inorg. Chem.* **2011**, *16*, 1035.
(6) Zeitoun-Ghandour, S.; Charnock, J. M.; Hodson, M. E.; Leszczyszyn, O. I.; Blindauer, C. A.; Sturzenbaum, S. R. *FEBS J.* **2010**, *277*, 2531.
(7) Stillman, M. J. *Coord. Chem. Rev.* **1995**, *144*, 461.
(8) Sutherland, D. E. K.; Stillman, M. J. *Metallomics* **2011**, *3*, 444.
(9) Robbins, A. H.; McRee, D. E.; Williamson, M.; Collett, S. A.; Xuong, N. H.; Furey, W. F.; Wang, B. C.; Stout, C. D. *J. Mol. Biol.* **1991**, *221*, 1269.
(10) Messerle, B. A.; Schaffer, A.; Vasak, M.; Kagi, J. H. R.; Wuthrich, K. *J. Mol. Biol.* **1990**, *214*, 765.
(11) Messerle, B. A.; Schaffer, A.; Vasak, M.; Kagi, J. H. R.; Wuthrich, K. *J. Mol. Biol.* **1992**, *225*, 433.
(12) Kramer, K. K.; Zoelle, J. T.; Klaassen, C. D. *Toxicol. Appl. Pharmacol.* **1996**, *141*, 1.
(13) Kramer, K. K.; Liu, J.; Choudhuri, S.; Klaassen, C. D. *Toxicol. Appl. Pharmacol.* **1996**, *136*, 94.
(14) Uchida, Y.; Takio, K.; Titani, K.; Ihara, Y.; Tomonaga, M. *Neuron* **1991**, *7*, 337.
(15) Quaife, C. J.; Findley, S. D.; Erickson, J. C.; Froelick, G. J.; Kelly, E. J.; Zambrowicz, B. P.; Palmiter, R. D. *Biochemistry* **1994**, *33*, 7250.
(16) Quaife, C. J.; Kelly, E. J.; Masters, B. A.; Brinster, R. L.; Palmiter, R. D. *Toxicol. Appl. Pharmacol.* **1998**, *148*, 148.
(17) Calderone, V.; Dolderer, B.; Hartmann, H.-J.; Echner, H.; Luchinat, C.; Del-Bianco, C.; Mangani, S.; Weser, U. *Proc. Natl. Acad. Sci. U.S.A.* **2005**, *102*, 51.
(18) Arseniev, A.; Schultze, P.; Worgotter, E.; Braun, W.; Wagner, G.; Vasak, M.; Kagi, J. H. R.; Wuthrich, K. *J. Mol. Biol.* **1988**, *201*, 637.
(19) Schultze, P.; Worgotter, E.; Braun, W.; Wagner, G.; Vasak, M.; Kagi, J. H. R.; Wuthrich, K. *J. Mol. Biol.* **1988**, *203*, 251.
(20) Zangger, K.; Oz, G.; Otvos, J. D.; Armitage, I. M. *Protein Sci.* **1999**, *8*, 2630.
(21) Wang, H.; Zhang, Q.; Cai, B.; Li, H.; Sze, K.-H.; Huang, Z.-X.; Wu, H.-M.; Sun, H. *FEBS Lett.* **2006**, *580*, 795.
(22) Chan, J.; Huang, Z.; Watt, I.; Kille, P.; Stillman, M. J. *Can. J. Chem.* **2007**, *85*, 898.
(23) Briggs, R. W.; Armitage, I. M. *J. Biol. Chem.* **1982**, *257*, 1259.
(24) Li, H.; Otvos, J. D. *Biochemistry* **1996**, *35*, 13929.
(25) Salgado, M. T.; Stillman, M. J. *Biochem. Biophys. Res. Commun.* **2004**, *318*, 73.
(26) Ngu, T. T.; Easton, A.; Stillman, M. J. *J. Am. Chem. Soc.* **2008**, *130*, 17016.
(27) Nielson, K. B.; Atkin, C. L.; Winge, D. R. *J. Biol. Chem.* **1985**, *260*, 5342.
(28) Green, A. R.; Presta, A.; Gasyna, Z.; Stillman, M. J. *Inorg. Chem.* **1994**, *33*, 4159.
(29) Cai, W.; Stillman, M. J. *J. Am. Chem. Soc.* **1988**, *110*, 7872.

(30) Ngu, T. T.; Dryden, M. D. M.; Stillman, M. J. *Biochem. Biophys. Res. Commun.* **2010**, *401*, 69.
(31) Gehrig, P. M.; You, C.; Dallinger, R.; Gruber, C.; Brouwer, M.; Kagi, J. H. R.; Hunziker, P. E. *Protein Sci.* **2000**, *9*, 395.
(32) Sutherland, D. E. K.; Stillman, M. J. *Biochem. Biophys. Res. Commun.* **2008**, *372*, 840.
(33) Ngu, T. T.; Krecisz, S.; Stillman, M. J. *Biochem. Biophys. Res. Commun.* **2010**, *396*, 206.
(34) Rigby-Duncan, K. E.; Stillman, M. J. *FEBS J.* **2007**, *274*, 2253.
(35) Palumaa, P.; Eriste, E.; Njunkova, O.; Pokras, L.; Jornvall, H.; Sillard, R. *Biochemistry* **2002**, *41*, 6158.
(36) Ngu, T. T.; Stillman, M. J. *J. Am. Chem. Soc.* **2006**, *128*, 12473.
(37) Krezel, A.; Maret, W. *J. Am. Chem. Soc.* **2007**, *129*, 10911.
(38) Rigby-Duncan, K. E.; Kirby, C. W.; Stillman, M. J. *FEBS J.* **2008**, *275*, 2227.
(39) Sutherland, D. E. K.; Willans, M. J.; Stillman, M. J. *Biochemistry* **2010**, *49*, 3593.
(40) Meloni, G.; Polanski, T.; Braun, O.; Vasak, M. *Biochemistry* **2009**, *48*, 5700.
(41) Palumaa, P.; Njunkova, O.; Pokras, L.; Eriste, E.; Jornvall, H.; Sillard, R. *FEBS Lett.* **2002**, *527*, 76.
(42) Feng, W.; Cai, J.; Pierce, W. M.; Franklin, R. B.; Maret, W.; Benz, F. W.; Kang, Y. J. *Biochem. Biophys. Res. Commun.* **2005**, *332*, 853.
(43) Mason, A. Z.; Perico, N.; Moeller, R.; Thrippleton, K.; Potter, T.; Lloyd, D. *Mar. Environ. Res.* **2004**, *58*, 371.
(44) Maret, W.; Larsen, K. S.; Vallee, B. L. *Proc. Natl. Acad. Sci. U.S.A.* **1997**, *94*, 2233.
(45) Meloni, G.; Sonois, V.; Delaine, T.; Guilloreau, L.; Gillet, A.; Teissie, J.; Faller, P.; Vasak, M. *Nat. Chem. Biol.* **2008**, *4*, 366.
(46) Chan, J.; Merrifield, M. E.; Soldatov, A. V.; Stillman, M. J. *Inorg. Chem.* **2005**, *44*, 4923.
(47) Ejnik, J. W.; Munoz, A.; DeRose, E.; Shaw, F. III; Petering, D. H. *Biochemistry* **2003**, *42*, 8403.
(48) Felitsyn, N.; Peschke, M.; Kebarle, P. *Int. J. Mass spectrom.* **2002**, *219*, 39.
(49) Kebarle, P.; Verkerk, U. H. *Mass Spectrom. Rev.* **2009**, *28*, 898.
(50) Boulanger, Y.; Armitage, I. M. *J. Inorg. Biochem.* **1982**, *17*, 147.
(51) Ellis, P. D. *Science* **1983**, *221*, 1141.
(52) Iranzo, O.; Jakusch, T.; Lee, K.-H.; Hemmingsen, L.; Pecoraro, V. L. *Chem.—Eur. J.* **2009**, *15*, 3761.
(53) Jensen, L. T.; Peltier, J. M.; Winge, D. R. *J. Biol. Inorg. Chem.* **1998**, *3*, 627.
(54) Li, Y.; Maret, W. *J. Anal. At. Spectrom.* **2008**, *23*, 1055.
(55) Boulanger, Y.; Armitage, I. M.; Miklossy, K.-A.; Winge, D. R. *J. Biol. Chem.* **1982**, *257*, 13717.
(56) Stillman, M. J.; Cai, W.; Zelazowski, A. J. *J. Biol. Chem.* **1987**, *262*, 4538.
(57) Willner, H.; Vasak, M.; Kagi, J. H. R. *Biochemistry* **1987**, *26*, 6287.
(58) Chen, X.; Chu, M.; Giedroc, D. P. *Biochemistry* **1999**, *38*, 12915.
(59) Giedroc, D. P.; Chen, X.; Pennella, M. A.; LiWang, A. C. *J. Biol. Chem.* **2001**, *276*, 42322.
(60) Zhang, B.; Georgiev, O.; Hagmann, M.; Gunes, C.; Cramer, M.; Faller, P.; Vasak, M.; Schaffner, W. *Mol. Cell. Biol.* **2003**, *23*, 8471.
(61) Palacios, O.; Polec-Pawlak, K.; Lobinski, R.; Capdevila, M.; Gonzalez-Duarte, P. *J. Biol. Inorg. Chem.* **2003**, *8*, 831.
(62) Salgado, M. T.; Bacher, K. L.; Stillman, M. J. *J. Biol. Inorg. Chem.* **2007**, *12*, 294.
(63) Knipp, M. *Curr. Med. Chem.* **2009**, *16*, 522.
(64) Hagrman, D.; Goodisman, J.; Dabrowiak, J. C.; Souid, A.-K. *Drug Metab. Dispos.* **2003**, *31*, 916.
(65) Knipp, M.; Karotki, A. V.; Chesnov, S.; Natile, G.; Sadler, P. J.; Brabec, V.; Vasak, M. *J. Med. Chem.* **2007**, *50*, 4075.
(66) Casini, A.; Karotki, A.; Gabbiani, C.; Rugi, F.; Vasak, M.; Messori, L.; Dyson, P. J. *Metallomics* **2009**, *1*, 434.
(67) Karotki, A. V.; Vasak, M. *J. Biol. Inorg. Chem.* **2009**, *14*, 1129.
(68) Karotki, A. V.; Vasak, M. *Biochemistry* **2008**, *47*, 10961.
(69) Manso, Y.; Adlard, P. A.; Carrasco, J.; Vasak, M.; Hidalgo, J. *J. Biol. Inorg. Chem.* **2011**, *16*, 1103.
(70) Manso, Y.; Serra, M.; Comes, G.; Giralt, M.; Carrasco, J.; Cols, N.; Vasak, M.; Gonzalez-Duarte, P.; Hidalgo, J. *J. Neurosci. Res.* **2010**, *88*, 1708.